Chapter III

Phenalenone Based Colorimetric and Fluorometric pH Indicators for Alkaline Solution

Abstract

The synthesis, characterization and application of two phenalenone based fluorescent compounds, 9-(4-hydroxyphenyl amino)-1-oxo phenalenone (**1**) and 2, 2-difluoro-3-(4-hydroxyphenyl)-2-bora-3-aza-1-oxophenalene (**2**) have been described. Compounds **1** and **2** are capable of working as colorimetric and fluoremetric pH sensors for alkaline solution in ethyl alcohol-water (1:1, v/v) system. The pKa value determined for these dyes are in the range of 7-9 and shows that the phenol group substituent is responsible for fluorescence emission quenching via photo induced electron transfer (PET) mechanism.

III.1. Introduction

The rational design and development of different systems and methods for selective detection of ions have gained considerable attention in current research field [1-4]. Along with the enhancing requirement of developing metal ion sensors the recognition of H^+ ion has also emerged as a subject demanding wide importance. The pH or the active H^+ ion concentration is important for the regulation of biological systems such as cell growth, transportation of ion, enzymatic activity, agriculture, biopharmaceutical industry, medicine and water treatment [5,6]. Abnormality in intracellular pH in living organism causes cancer and Alzheimer disease [7, 8]. Several techniques have been adopted for sensing the pH of working solution including polyethylimine based quantum dots (QD) containing silver nanoparticles (Ag NPs) as efficient pH sensing probes [9]. Several QD based pH sensors have been demonstrated, where the sensor can act in different pH ranges, for example pH 7.1–8.5 for CdSe–ZnS core–shell QDs [10], pH 4.0–8.0 for mercapto acetic acid-capped CdSe/ZnSe/ZnS QDs, [11]. Beside the development of QDs, nanoscale based pH sensors include modified nanoparticles [12-15]. These sensors have their limitations to be used as strong alkaline pH sensors as they are effective for acidic pH range and in slightly basic pH value up to 8.5. Potentiometric pH sensors based on redox compounds have been reported by Laftte *et al*. [16]. However, redox active pH sensors often lack the advantage of stability due to potential drift, which require very frequent calibration [17]. In practical field the potentiometric application of Glass electrodes for pH determination is very common because of high sensitivity and stablity to environmental conditions. In spite of this, they too undergo instability towards potential drift caused by high activity of H^+ ion. Further strong alkaline conditions also make them unsuitable for repeated use owing to 'alkali error' [18, 19]. To eliminate the drawbacks of potentiometric sensing, amperometric pH sensors had been introduced in the past. These sensors utilize polymer films [20]; organic redox molecules such as quinine, often used for functionalise the modified carbon surface [21, 22]. Before the development of electrochemical aspects NMR techniques had been used as authentic tool for pH determination [23]. Simultaneous efforts have been given for the development of optical pH sensors in more than last 30 years [24].

Optical pH indicators show reversible changes in spectral features, hence absorption and emission spectroscopy are adopted as the most reliable tool due to easy operation and high sensibility [25-29]. Hitherto, several pH sensors have been reported based on 1, 8- naphthalimide derivative [30], rhodamine [31], carbazole derivative [32] etc. Recent developments are reported with the application of aza boron dipyrromethene (aza-BODIPY) compounds [33-35]. On the other hand, only few indicators are popular for strongly alkaline medium (> pH 10) because of their low stability and wide interval of colour change [36]. Thus, dual colorimetric and fluorometric pH probes for alkaline solutions could be useful, particularly for the pH estimation of alkaline industrial waste [37]. Schäferling and Zhang have recently reported two Förster resonance energy transfer (FRET) based sensors but the upper limit of the detectable pH was 9 and no sharp colour change was observed in visible light;[38, 39] suggesting that plenty of scope remains for new building blocks to be explored in this context.

It has been always challenging to introduce new building blocks as fluoremetric and colorimetric dual probes for any sensing application [40]. There are mainly three (Litmus, Delphinidin, Cyaniding) naturally occurring popular pH indicators, derived from plant extracts, but none of those shows a sharp colour change in the highly basic medium [41]. Moreover, these indicators do not act as colorimetric and fluorometric dual probes. Same problem persists for the other dye based pH indicators such as Bromocresol green, Cresol red, Thymol blue etc. Phenalenone is also a naturally occurring compound, available from the plant extract, [42] but the added advantage of this compound is its easy synthesis and convenient functionalization procedure. Herein we are describing the synthesis and application of two phenalenone based fluorophores, 9-(4-hydroxyphenyl)-1-oxophenalene (**1**) and 2,2-difluoro-3-(4-hydroxyphenyl)-2-bora-3-aza-1-oxophenalene (**2**), as reversible pH indicators. Our previous work described the first application of a neutral phenalenone (PLY) based molecule as a selective chemosensor for iodide ion [43]. Here sensors **1** and **2** have been designed by the combination of 4-aminophenol and phenalenone subunit. Phenol group when deprotonated to phenoxide ion can act as a photo induced electron transfer (PET) group by showing quenching in emission intensity. Gareis *et al*. for the first time demonstrated phenoxide group as PET quencher by means of boron dipyrromethene (BODIPY)

[44]. Later Kiloran *et al*. reported phenol substituted aza-BODIPY dyes for pH sensing where phenoxide anion has led to photo induced electron transfer (PET) [45]. Halogenated phenol containing molecules are also reported as pH sensors where both phenol and ammine functional act as efficient PET groups [46]. Design of compound **1** has been inspired by this report on pH sensing shown by phenols attached with different fluorophores. Design of compound **2** has been dictated by the success of BODIPY framework as fluorescent indicators [47, 48]. Thus we anticipate compounds **1** and **2** (Scheme III.1), to show pH dependent emission changes by PET while proposing ample opportunity to investigate the additional changes in the photochemical properties imparted by the combination of phenol and the phenalenone moiety.

III.2. Results and discussion

III.2.1. Synthesis

The molecule, 9-(4-hydroxyphenyl amino)-1-oxo phenalenone (**1**) has been prepared by modifying the procedure earlier reported by Yang *et al*. in 50% yield [49]. Similar Ply derivatives have been reported by the same group, where *p*-methoxy aniline has been chosen as the substituent. These compounds upon boronation are found to show aggregation induced emission property [50].

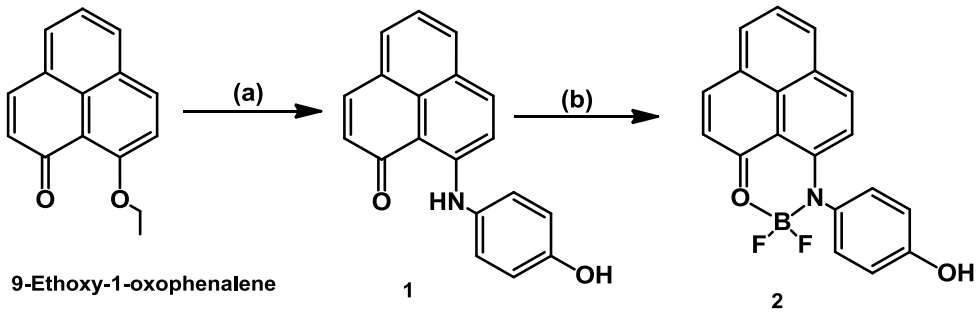

Scheme III.1. Schematic route to synthesize **1** and **2**: (a) *p*-aminophenol in Methanol-1, 2-dichloromethane (1:1); (b) $BF_3.Et_2O$, 1, 2-dichloromethane.

In place of *p*-methoxy aniline we have chosen *p*-amino phenol. Since *p*-amino phenol is highly soluble in protic polar solvent, methanol−1, 2-dichloromethane (1:1) solvent mixture has been taken as the reaction medium. Further reaction of **1** with $BF_3.Et_2O$ in 1, 2-dichloroethane gives compound **2** in 73% yield [51] (Scheme III.1). Both these compounds have been characterized by NMR spectroscopy, ESI Mass spectroscopy and elemental analysis. The ^1H NMR, ^{13}C NMR and ESI Mass spectra of these compounds are given in the experimental section (Fig.III.22-28). The ESI mass

spectral characterization of **1** and **2** has been carried out in methanol. The mass spectra of **1** shows molecular ion peak at m/z 288.15 which corresponds to (**1**+H^+) and that of **2** consists of a signal at m/z 316.18, corresponding to (**2**-HF)$^+$, which is possibly generated due to the fragmentation of the –BF2 unit attached with the –NH group and carbonyl O-atom.

III.2.2. Electronic spectra of sensors 1 and 2

The UV-visible spectra of **1** and **2** have been recorded in ethanol-water (1:1, v/v) solution. In the UV-visible absorption spectra of **1**, absorption peaks at 253 nm, 355 nm and 470 nm are observed along with a shoulder at 442 nm (concentration of **1** = $5x10^{-6}$ M) (black solid line in Fig.III.1). For compound **2** although the overall absorption spectral feature is similar to **1**, the peaks are observed to appear slightly blue shifted than **1**. In the UV-visible spectra of **2**, absorption peaks at 244 nm, 365 nm, 436 nm and 462 nm are observed ($5x10^{-6}$ M, ethanol-water, 1:1, v/v) (blue dotted line in Fig.III.1).

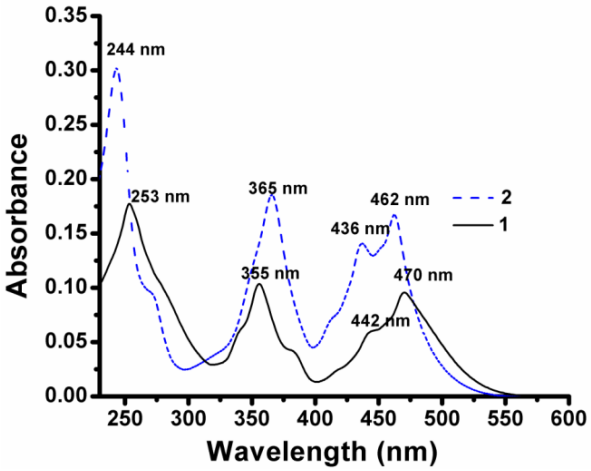

Fig.III.1. UV-visble spectra of **1** and **2** in ethanol-water (1:1 v/v).

III.2.3. Fluorescence emission spectra of sensors 1 and 2

The fluorescence emission spectra of these compounds have been studied in ethanol-water (1:1, v/v) mixed solvent medium. When $5x10^{-6}$ M solutions of **1** and **2** are excited at a wavelength 265 nm, sharp emission signals at 305 and 302 nm respectively are observed (Fig.III.2).

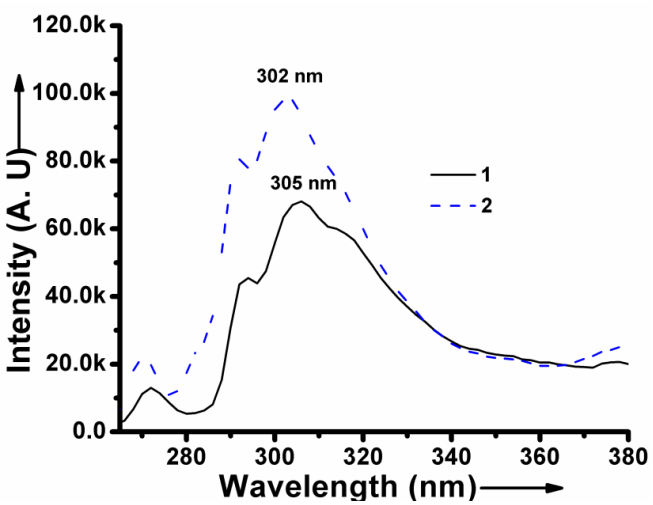

Fig.III.2. Fluorescence emission spectra of **1** and **2** in ethanol-water mixed solvent (1:1 v/v).

Although the overall feature of the emission spectra of compounds **1** and **2** are similar, from Fig.III.2, it is observed that the emission intensity for **2** (blue dotted line in Fig.III.1) is greater than that of compound **1** (black solid line in Fig.III.2).

During fluorescence experiments, when a solution of **1** is excited at higher wavelengths (367 nm, 438 nm and 468 nm) some very weakly emissive peaks are observed in the region 500-650 nm, but upon exciting the solutions of compounds **1** at 250 nm, highly intense emission peaks are observed at 306 nm (Fig.III.3).

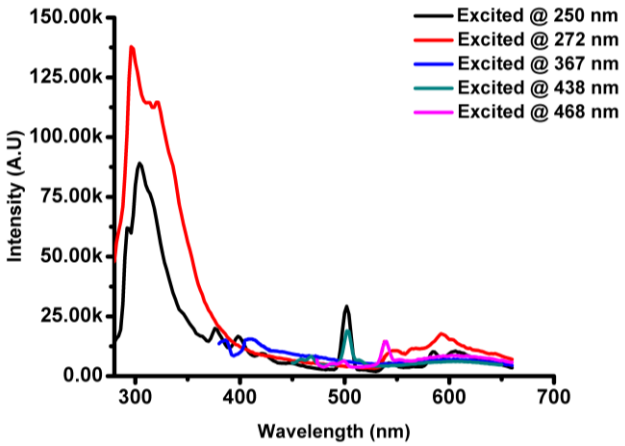

Fig.III.3. Emission spectra of **1** excited at different wavelengths (no absorption peak corresponding to 272 nm is seen in electronic absorption spectra and chosen arbitrarily, [**1**] = $7x10^{-6}$ M). Concentration of the sensor **1** was kept at $5x10^{-6}$ M in ethanol).

Emission intensities in different solvents have also been investigated. Sharp reduction of emission intensities has been observed with the increase in solvent polarity (Fig.III.4), which implies that a PET mechanism could be operative in the molecules [52].

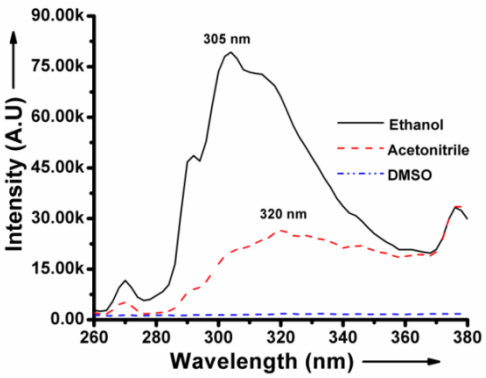

Fig.III.4. Fluorescence emission spectra of **1** (5 x 10^{-6} M) in different solvents.

Table III.1 Change in emission intensity of **1** with polarity of solvents

Solvent	Dielectric constant	Intensity (A.U)
Etahnol	24.5	79286
Acetonitrile	37.5	20078
Dimethyl Sulfoxide (DMSO)	46.7	1424

III.2.3.1. Quantum yield determination of 1 and 2

The fluorescence quantum yields (Φ_f) of both the compounds **1** and **2** have been calculated using equation III. 1 [53, 46].

$$\Phi_f \text{ (sample)} = (A_{sample}/ A_{standard}) \times (OD_{standard})/(OD_{sample}) \times \Phi_f \text{ (standard)}. \quad \text{(III. 1)}$$

The fluorescence quantum yields (Φ_f) for compound **1** (0.075) and **2** (0.0896) have been calculated from integrating emission area under the fluorescence spectra of the respective compounds with the above equation at pH 7.2. Aqueous solution of Tryptophan (λ_{emm} = 300-380 nm, Φ_f = 0.14 at pH 7.2 in aqueous medium) has been used as standard for Φ_f calculations. Although various fluorophores are reported in literature with high Φ_f values, a correlation can be drawn with recently reported efficient pH probes. Yan *et al.* have reported a series of structural analogue of **2**, where the secondary amine is linked with either alkyl or aryl groups. There in the compounds with phenyl, *p*-methoxyphenyl and *p*-cyanophenyl group substituents show Φ_f values 0.006, 0.008 and 0.003 respectively, in THF solution [54]. The higher Φ_f values for probes **1** and **2** (0.075 and 0.0896 respectively) add extra value to their

emission property. Novel pH sensors with rhodamine fluorophore and dichlorophenol as PET group show Φ_f of 0.084 in ethanol-water system (1:1, v/v), which is close to the Φ_f value of **2**. Recent pH sensor with aminoperylene bisimide as fluorophore and dichlorophenol as PET group has a Φ_f of 0.052 in acid medium and <0.01 in basic medium [55]. A series of pH sensors based on naphthalimide as fluorophore and 2, 6-disubstituted phenol as PET group are reported with Φ_f value in the range of 0.03 to 0.1 in basic and acid medium respectively [46].

III.3. pH sensing property of 1 and 2

In order to investigate the pH responsive property of 1 and 2, the UV-visible and fluorescence spectra of these compounds have been recorded in 1:1 ethanol/water mixed solvent medium in presence of 0.1 M HEPES buffer. HEPES buffered solutions with various pH values ranged from 1.0 to 13.5 in DMF/H_2O (9:1, v/v) have been used for a nonbiological pH sensor by Zhu *et al*. [56]. While recording the UV-visible spectra of **1** in different pH a new set of peaks are observed at 516, 400, 380 and 289 nm at pH 11 (Fig.III.5).

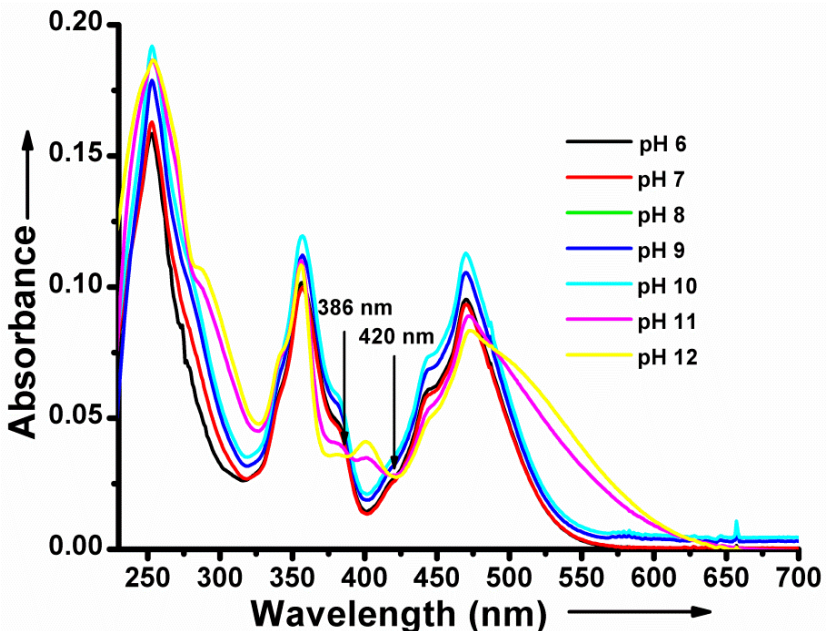

Fig.III.5. Change in UV-visible absorption spectra of **1** (5 x10^{-6} M) at different pH in ethanol-water (1:1, v/v) mixture containing 0.1 M HEPES buffer solution.

Appearance of new peaks clearly indicates the formation of a new species (phenolate) in the representative pH. Isobestic points have been clearly seen in the UV at 386 nm and 420 nm which indicates that two species are in equilibrium in the solution. A sigmoidal plot with excellent fit is obtained when absorbance has been

plotted against pH (Fig.III.6), indicating that UV based pH measurement is possible over the pH range 6 to 12.

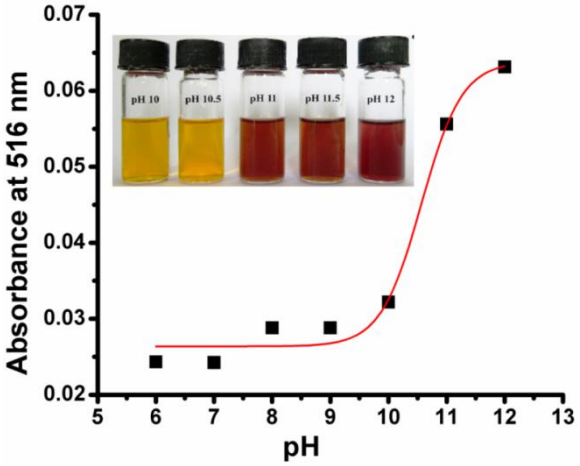

Fig.III.6. Plot of absorbance at 516 nm versus pH for **1** showing a sigmoidal change in absorbance value with increase in pH; inset figure shows visible colour change of **1** at different pH.

When the absorption spectra have been recorded at lower pH i.e. in acidic region, no significant changes are observed, but at high pH region or basic region a broad band at 516 nm is seen. The solution also changes colour from yellow to red at high basic region. At pH 11 this sharp change in colour is detectable with naked eye (Fig.III.6 inset). The structure of **1** suggests that there are two possible dissociable sites in alkaline solution, one is the phenol group and the other is the amine group. To find out the actual site compound **1** has been converted to compound **2** by treatment of $BF_3.Et_2O$. The spectral changes of **2** have also been investigated with change in pH of solution with the same experimental conditions. Promising spectral changes have been observed for compound **2** with the appearance of a new peak at 516 nm along with another small peak at 290 nm (Fig.III.7) at pH 10.

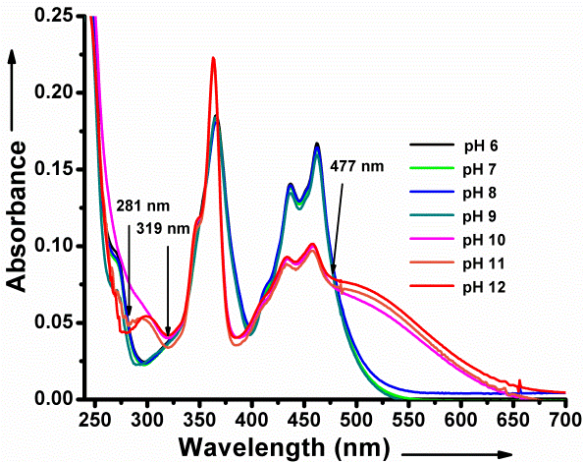

Fig.III.7. (a) Changes in electronic absorption spectra of **2** at different pH of solution ($5x10^{-6}$ M, 0.1 M HEPES buffer, 1:1 ethanol-water, v/v); (b) plot of absorbance versus pH of solution for **2**.

In the electronic spectra of **2** at different pH, isosbestic points at 281 nm, 319 nm and 477 nm are observed. Similar to receptor **1**, sensor **2** also shows visible colour change at pH 10 (inset in Fig.III.8). Also the plot of absorbance at different pH vs. pH gives a sigmoidal curve for **2** (Fig.III.8).

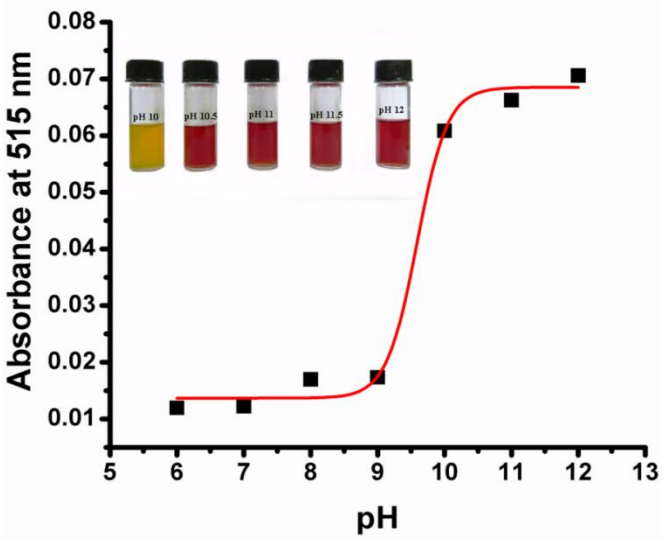

Fig.III.8. Plot of absorbance versus pH of solution for **2**; inset shows visible colour change of **2** at different pH.

This indicates that the spectroscopic and visible colour change may arise due to deprotonation of the phenol group to phenoxide ion.

The pH responsive ability of these two receptors has also been investigated through fluorescence experiments. In fluorescence experiments quenching in emission intensity is observed when the pH of probe solutions is gradually shifted from acidic to basic region. Increase in emission intensity with the increase in H^+ concentration is known for photo induced electron transfer (PET) based sensors [51].

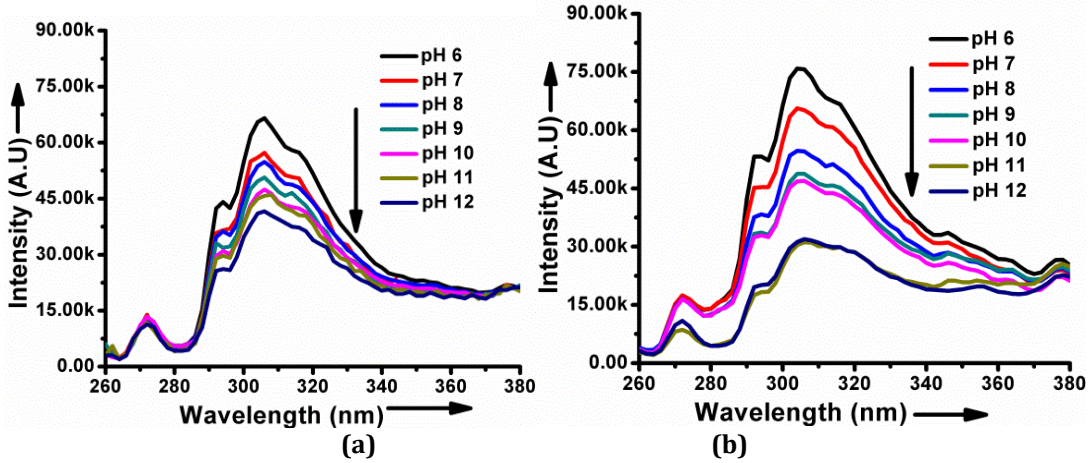

Fig.III.9. Fluorescence emission spectral changes of **1** (a) and **2** (b) at different pH in 1:1 ethanol/water (v/v) in mixture containing 0.1 M HEPES buffer solution.

The emission intensity of **1** is gradually decreased with increase in pH of the solutions [Fig.III.9a]. Similar quenching in emission intensity is observed for sensor **2** when the pH of the solution has gradually been increased from 6 to 12 (Fg.III.9b). The above figures show that this change finally attains a constant value above pH 11. Excellent linear fits in the pH range from 7 to 12 for **1** and from 6 to 11 for **2** shows that they can be used as fluorescent intensity based pH sensors in the mentioned pH windows (Fig.III.10a and b).

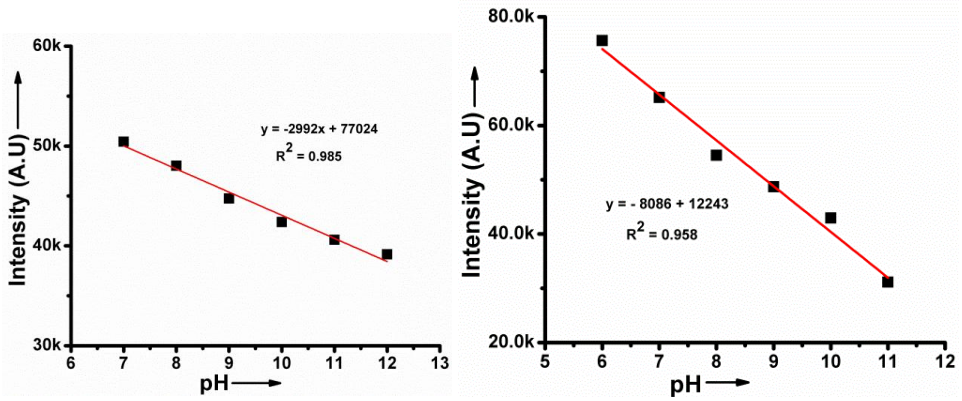

Fig.III.10. Plot of fluorescence intensity *vs* pH of solution for **1** (a) and **2** (b).

Absence of bathochromic or hypsochromic shifts in the emission spectra implies that the sensing could be PET driven. The pH responsive property of **1** and **2** is visually observable in highly basic medium (> pH 11 for **1** and > pH 10.5 for **2**).

III.3.1. Calculation of pKa of 1 and 2

The acidity constant pKa of **1** and **2** have been calculated using Henderson-Hasselbalch Equation (equation III. 2) [57] with the help of fluorescence emission data, where 'F' is the observed integrated emission intensity at a fixed wavelength, 'F_{max}' and 'F_{min}' are the maximal and minimal integrated emission intensity, respectively. The Henderson-Hasselbalch equation is shown below:

$$pH - pKa = \log (F_{max} - F/F - F_{min}) \ldots\ldots\ldots\ldots (III.\ 2.)$$

From the intercept at the Y-axis the pKa value is directly obtained. The pKa Value obtained for **1** is 7.1, which is close to the pKa values of phenolic compounds (Fig.III.11).

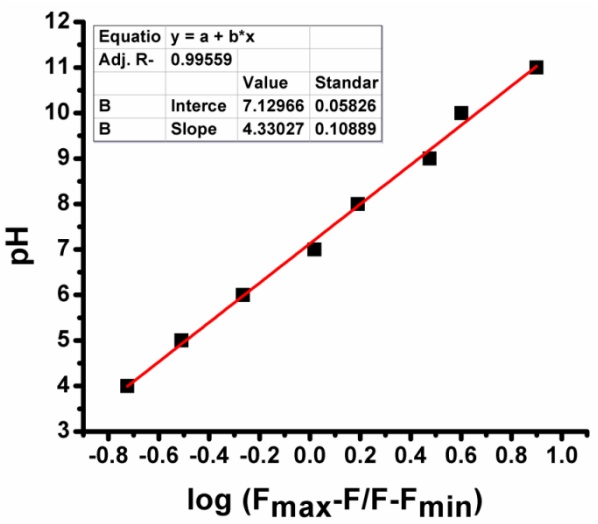

Fig.III.11. Plot of pH vs log (F_{max} – F/F – F_{min}) for the determination of pKa for **1**.

The pKa value for **2** has also been calculated with the same expression and the value is found to be 8.57, which is considerably greater than that of **1** (Fig.III.12).

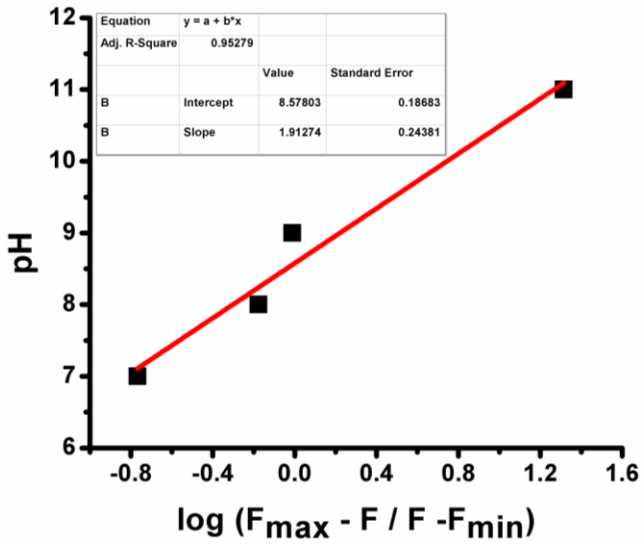

Fig.III.12. Plot of pH vs log (F_{max} – F/ F- $_{Fmin}$) for the determination of pKa of **2**.

This increased value in dissociation constant for **2** can be accounted for by the easier conversion of phenol to phenolate due to the introduction of a highly electron withdrawing –BF_2 group.

III.3.2. Switchable colorimetric and fluorometric pH sensing

Reversibility in basic form to acidic form and vice versa has been studied from 1:1 ethanol-water (v/v) solution for both the compounds. To investigate the reversibility of compounds **1** and **2**, 1 M HCl and 1M NaOH have been added alternatively to ethanol-water solution (1:1, v/v) of the sensors (5 x 10^{-5} M).

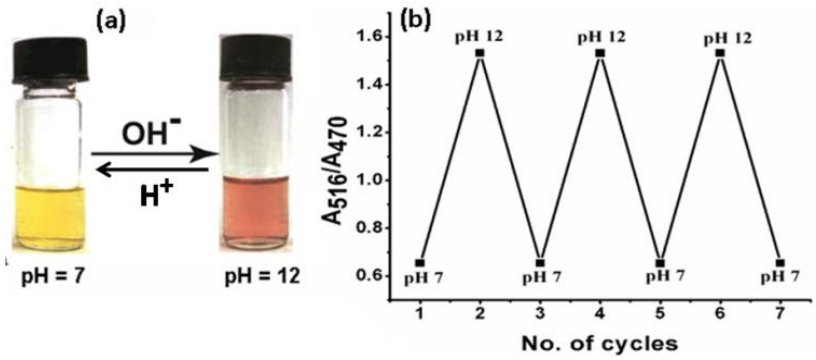

Fig.III.13. (a) Switchable colour change of **1** (5 x 10^{-5} M) within neutral and alkaline pH. (b) Reversible changes in the absorbance at 516 nm for **1** in ethanol-water (1/1, v/v) system within pH range 7-12.

The above figure (Fig.III.13) shows probe **1** can be reused up to 7 cycles upon alternate addition of base and acid. The reversibility has been verified by calculating the intensity ratios of the absorbance at constant wavelength for phenol form (470 nm) and phenolate form (516 nm). Similar behaviour has also been observed for compound **2** (Fig.III.14).

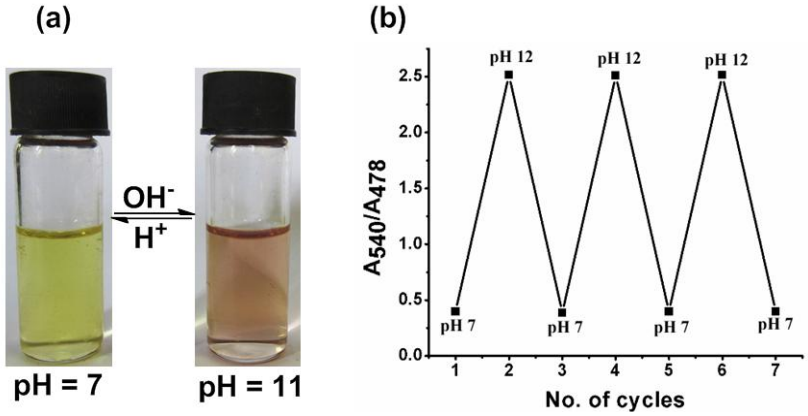

Fig.III.14. (a) Reversible colour changes of **2** upon alternate treatment of acid and base, (b) reversible changes in the absorbance at 540 nm for **2** (5 x 10^{-5} M) in ethanol-water (1/1, v/v) system within pH range 7-12.

The reversibility of property of **1** and **2** could be correlated when the emission intensity at 305 nm is reduced to a significant extent upon addition of aqueous NaOH solution with simultaneous change in fluorescent states from on to off (slightly residual emission can be observed in the off state). Later, upon addition of HCl the emission at 305 nm is almost regenerated to its initial position and "on" state restored (Fig.III.15(a) and (b)). Repeated addition of base and acids shows that the changes in emission are reproducible, thus the sensors can be reused.

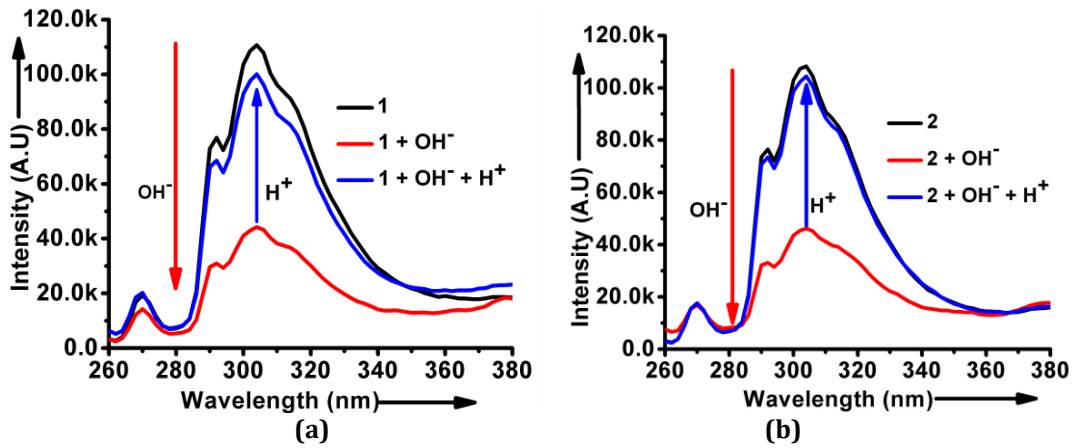

Fig.III.15. Switchable pH responsive property ("on-off" states)of probe **1** (a) and **2**(b); red trace: emission spectra of **1** and **2** after the addition of 0.1 M NaOH solution to a solution in ethanol-water (1:1, v/v, pH ~12) and blue trace is the emission spectra of **1** and **2** after the addition of 0.1 M NaOH solution followed by the addition of 0.1 M HCl solution ([**1**] and [**2**]: $5x10^{-6}$ M).

This suggests that both the probes **1** and **2** can be used as a reusable switchable colorimetric as well as fluoremetric sensors for alkaline pH. Colour of the phenolate state or the "off state" is persistent for several hours indicating the stability of the different forms in high alkaline solution.

Based up on this idea, a test has been conducted with alumina coated plates (Fig.III.16). The plate is able to demonstrate reversible colour change of the sensor in presence of interfering ions.

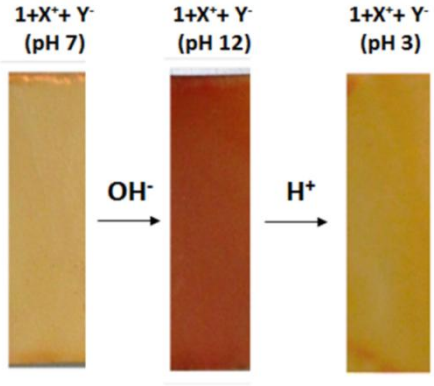

Fig.III.16. Chromatographic plate coated with 50 x 10^{-6} M of 1 (a) containing 50 equivalents of cation and anion solutions, (X^+= Co^{2+}, Ni^{2+}, Cu^{2+}, Zn^{2+}, Hg^{2+} and Pb^{2+} and Y^- = N_3^-, F^-, Cl^-, Br^-, I^-); (b) Same plate after eluting with NaOH solution (pH 12) and (c) the same plate after eluting with HCl solution (pH 3).

When the plate has been coated with **1** (Fig.III.16) and eluted with a solution of pH 12, containing interfering ions, colour changes to red (Fig.III.16b). The yellow colour of the plate has been again restored by eluting with dilute HCl solution (pH 3) (Fig.III.16c). This observation ensures the reusability of the sensor in acid and basic medium alternately.

III.3.3. Effect of added anions and cations on pH sensing by 1 and 2

The effect of presence of various interfering anion on the pH sensing ability of **1** and **2** would led us to know the practical applicability of these sensors in industrial wastes. Industrial wastes contain a number of common ions both cations and anions such as Co(II), Ni(II), Cu(II), Zn(II), Hg(II), Pb(II), F^-, Cl^-, Br^-, I^-, OAc^-. As these ions are strongly coordinating their presence in solution may alter the pH responsive property of the sensors. Effect of these ions on the emission intensity has been tested at the alkaline pH 8. Solutions of these ions (50 equivalents) have been added separately to a solution of **1** or **2** and the spectra are recorded by exciting at 250 nm.

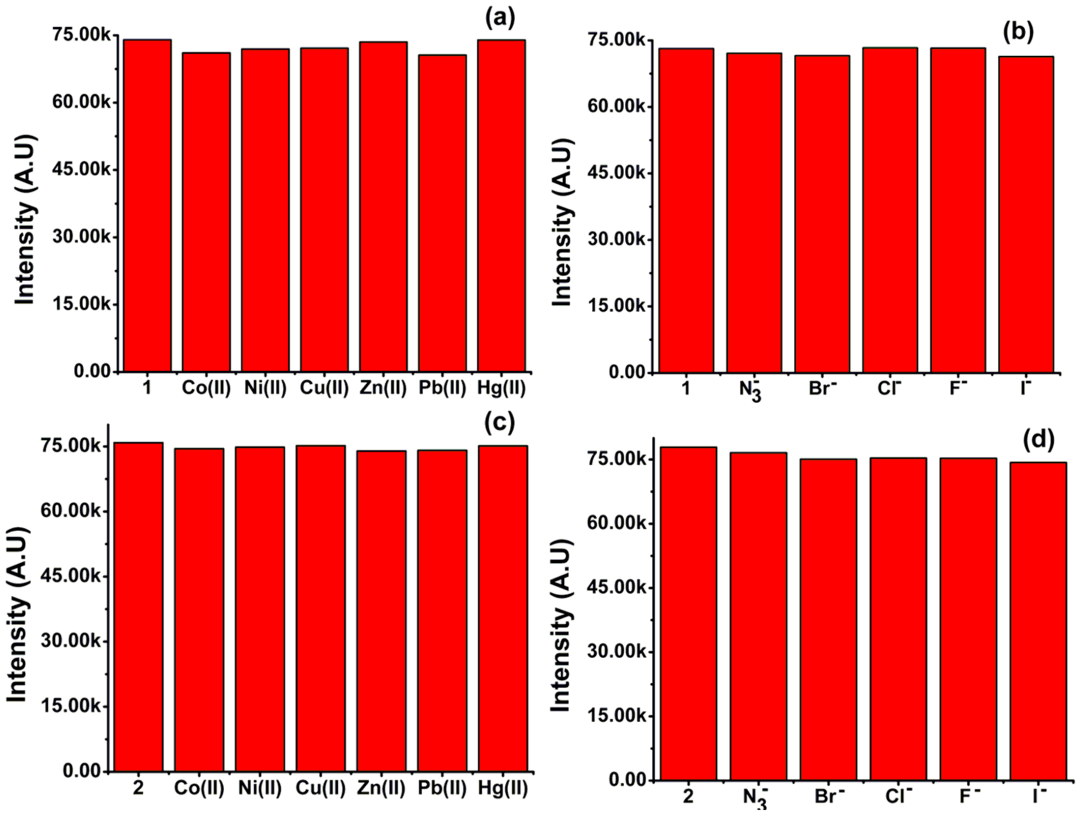

Fig.III.17. Effect of presence of cations and anions on emission of **1** (a and b) and **2** (c and d) (at pH 8). First columns indicate the initial emission intensity of **1**or **2** ($5x10^{-6}$ M) prior to the addition of 50 equivalent of perchlorate salts of cations or 50 equivalent of tetrabutyl ammonium salts of the anions (viz. F^-, Cl^-, Br^-, I^-) and sodium salt of N_3^- in 1:1 ethanol/water solution in HEPES buffer medium.

The almost equal heights of the columns in Fig.III.17 indicate that the presence of interfering ions in the working solution in a considerably high concentration does not affect the pH responsive property of **1** or **2** [58]. Therefore compounds **1** and **2** can be used as pH sensing probe even in the presence of different ions and also be applied for pH measurement of alkaline industrial wastes and other relevant purposes. These phenomena can be realized from the fact that due to the strong -N-

H-----O hydrogen bond, the hetero atoms of the phenalenone unit do not interact with other ions present in the test solution [59].

III.3.4. Mechanistic Aspects

III.3.4.1. ^{1}H NMR titration experiment

The mechanism of pH sensing phenomenon has been attempted to understand in light of ^{1}H NMR experiment. The proton NMR experiment of the dye **1** has been performed in DMSO-D6 (Fig.III.18).

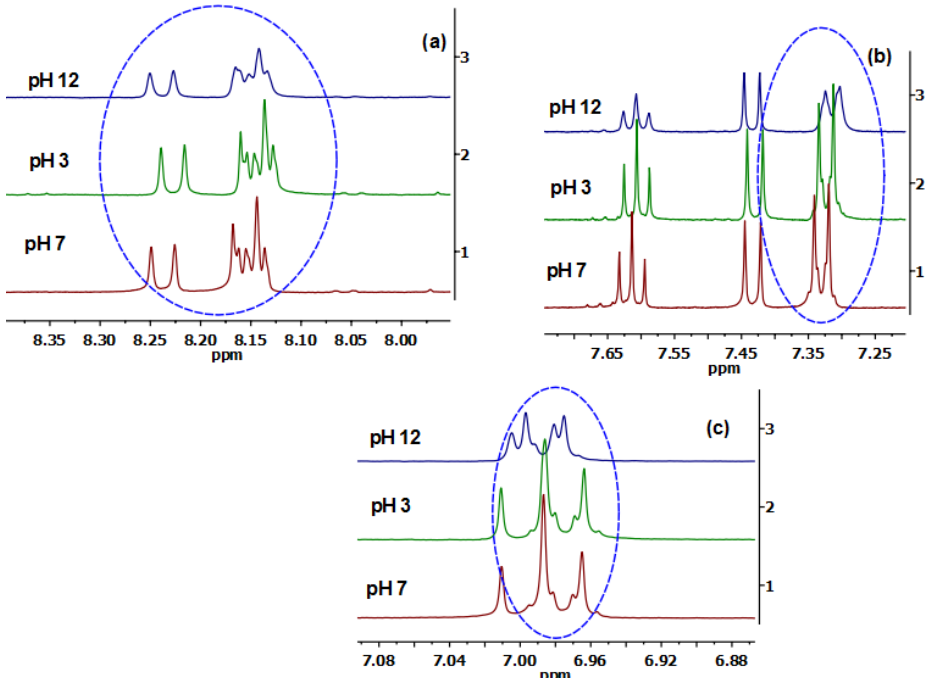

Fig.III.18. Expanded aromatic region of **1** at different pH.

The ^{1}H NMR spectra at pH 7 (red trace) has been recorded by placing a DMSO-D6 solution of **1** in an NMR tube. After recording at pH 7, 0.001 mL concentrated HCl has been added to make the pH ~3 and spectra have been recorded (green). Here the protons of aromatic ring in **1** are found to be shifted upon acidification. Again when the pH of working solution has been made ~12 by adding NaOH solution the aromatic protons are further shifted (shifts are shown in blue ellipsoids in aromatic regions). Changes in the ^{1}H NMR particularly at higher pH indicate the changes in the PLY framework.

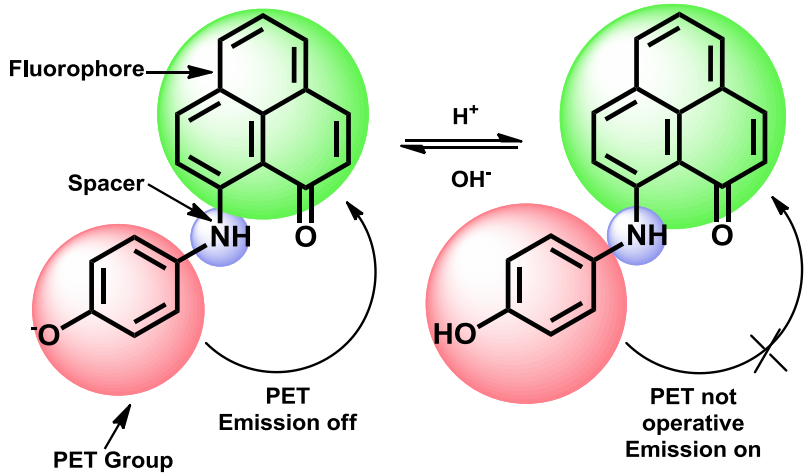

Scheme III.2. Schematic representation of the reversible conversion of **1** from anionic to neutral form.

The ^{1}H NMR experiment at different pH suggests that the phenol functional attached to the PLY fragment acts as a PET group. In the protonated state the photoelectron transfer from the –OH group is forbidden and thus PET is non operative and the molecule is expected to show fluorescence emission signals (Scheme III.2). But when the pH of the solution is increased phenol is deprotonated to phenoxide and thereafter transfers a photoelectron from the phenoxide ring to PLY ring via the –NH spacer arm. Hence emission intensity is decreased on increasing basicity of the solution.

III.3.4.2. DFT studies

DFT studies have been performed to understand the mechanism of pH sensing property of the receptor. The geometry of **1** has been fully optimized by DFT calculations at B3LYP level with 6-31G (d, p) basis set [62-66]. All the calculations have been carried out in gas phase. Geometry optimized structure of compound **1** is shown in Fig.III.19. The xyz-coordinates are given in the appendix.

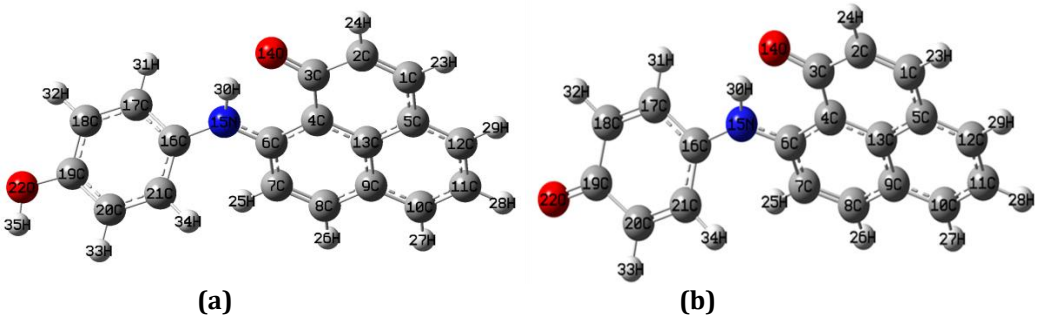

(a) **(b)**

Fig.III.19. Optimized structure of **1** in gas phase in (a) neutral form, (b) basic form (**1**$^{-}$).

Noncoplanar arrangement of the phenalenone and phenol units (Fig.III.28) rules out the possibility of intramolecular charge transfer (ICT) (angle between the phenalenone and phenyl planes is 46^0) as the main quenching mechanism.

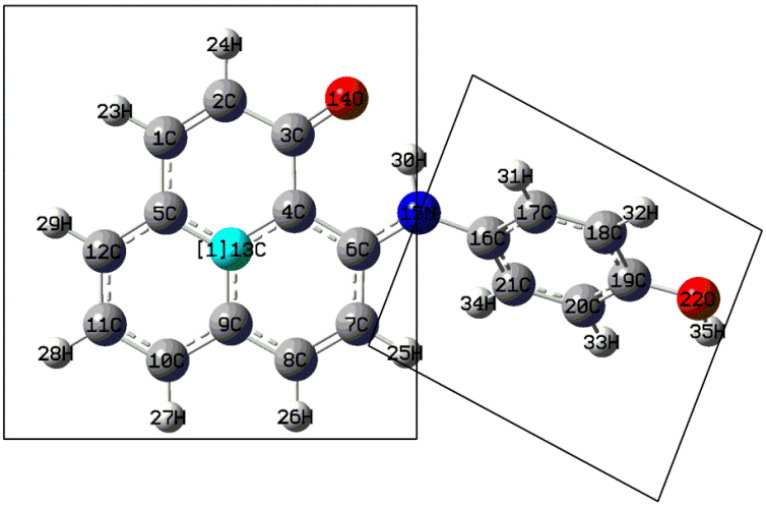

Fig.III.20. DFT optimized structure of **1** shows non-coplanar arrangement between the phenalenone and phenol planes.

Molecule **1** undergoes a pH-induced reversible electronic structural transformation between a conjugated (phenolate) and a nonconjugated (phenol) form (scheme III.3). Such a pH triggered structural modification shifts the HOMO–LUMO gap (Fig.III.21), indicated by the colour change of the solution and perturbations of the absorption peaks in the UV-visible spectra (absorption spectra shown in Fig.III.5 and III.7) beyond pH 11; supported by the bathochromic shift in UV at the same pH.

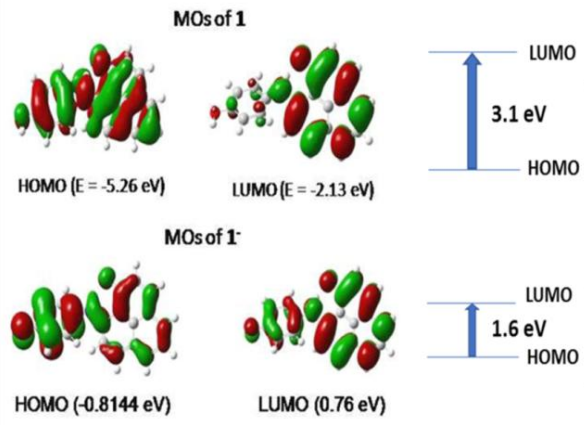

Species	E_{HOMO} (eV)	E_{LUMO} (eV)	ΔE
1	-5.26	-2.13	3.13
1⁻	-0.8144	0.76	1.58

Fig.III.21. HOMO-LUMO energy gap of phenolate and phenol forms of sensor **1**.

Table III.2. Selected bond lengths of **1** in neutral and anionic obtained from geometry optimization.

Compound	Bond	Bond lengths (Å)
1	6C-15N	1.34884
	15N-16C	1.34884
	15N-30H	1.39965
	19C-22O	1.04096
	19C-22O	1.25657
1^{-}	6C-15N	1.34884
	15N-16C	1.39965
	15N-30H	1.04096
	19C-22O	1.25657

Table III.3. Selected bond angles of **1** and its anionic form (**1**$^{-}$) derived from the optimized structure.

Compound	Angles	Bond angles (°)
1	<4C-6C-15N	119.03296
	<7C-6C-15N	121.9236
	<6C-15N-30H	111.70486
	<6C-15N-16H	128.6867
	<16C-15N-30H	119.5235
	<15N-16C-21C	122.70492
	<17C-16C-15N	118.54623
1^{-}	<4C-6C-15N	119.10272
	<7C-6C-15N	122.23876
	<6C-15N-30H	110.33813
	<6C-15N-16H	131.18593
	<16C-15N-30H	118.39765
	<15N-16C-21C	124.43943
	<17C-16C-15N	117.75535
	<31H-17C-16C	118.1789

Table III.4. Selected dihedral angles of **1** in neural and anionic state derived from the optimized structure.

Compound	Dihedral Angles	Dihedral Angles
1	<4C-6C-15N-16C	-172.57
	<7C-6C-15N-16C	9.37
	<6C-15N-16C-21C	45.42
	<6C-15N-16C-17C	-138.65
1^-	<4C-6C-15N-16C	-170.07
	<7C-6C-15N-16C	11.98
	<6C-15N-16C-21C	30.94
	<6C-15N-16C-17C	-152.63

The pH-induced changes in the molecular structure and electronic properties of the designed molecule suggest that the sensor molecule present a unique opportunity to fabricate single-molecule pH sensor based on its electrical switching function in four detectable channels (Scheme III.3). 1) Indication of phenol to H^+ interaction in ^1H NMR (Fig.III.18); 2) reduction of emission intensity with increase in solvent polarity (Fig.III.9); 3) non-planar arrangement between phenalenyl and phenol units in the optimized structures (Fig.III.19 and Tables III.2-III.4); 4) absence of bathochromic or hypsochromic shift in emission during variable pH experiment demonstrates that the PET mechanism is operative behind the pH sensing phenomena. Nevertheless, reduced HOMO-LUMO gap in case of phenolate form and corresponding bathochromic shift in absorption spectra indicates that an ICT mechanism is partially operative along with PET mechanism.

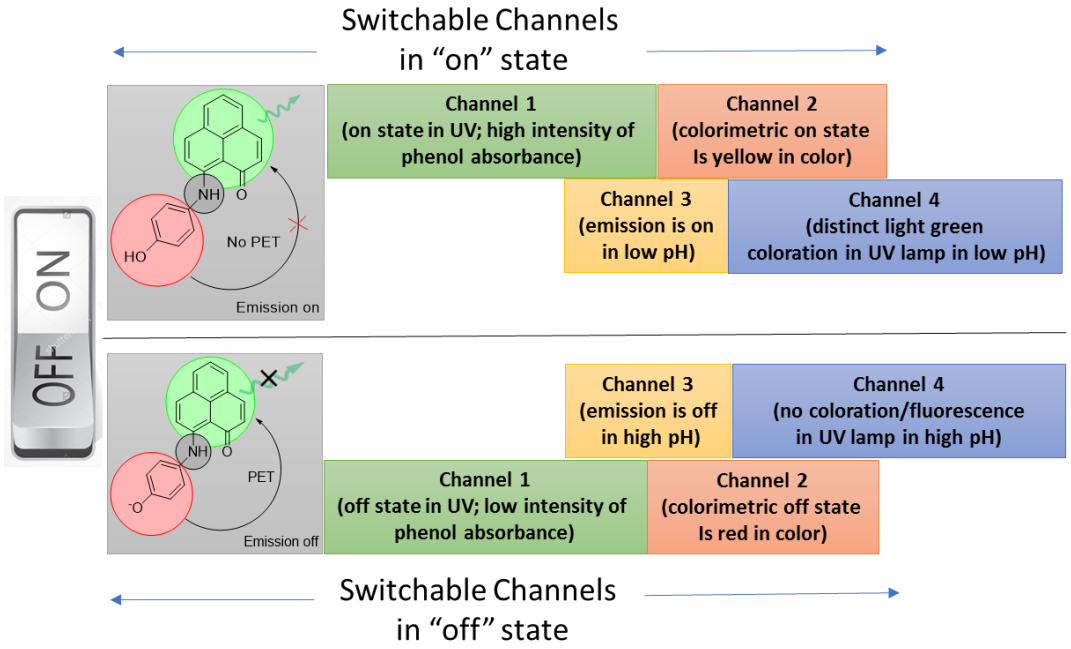

Scheme III.3. Schematic representation of colorimetric and emission change mechanism in sensor **1** resulting into switchable pH sensing in four detectable channels.

III.4. Conclusion

1. We have synthesized and characterized two newly designed pH sensing molecules **1** and **2** both containing PLY fragment as the fluorophore.

2. These two compounds have successfully introduced phenalenone moiety for colorimetric and fluorometric pH sensing by four detectable channels.

3. The sensors are able to show pH sensing property from neutral to highly basic window. Due to the colorimetric pH sensing property (Channel 2), compound **1** may be utilized as indicator for the detection of pH 11. On the other hand compound **2** can be used as an indication for the detection of pH of 10.5.

4. The presence of phenol group in the newly designed molecules facilitates the quenching of fluorescence emission in basic medium by a PET mechanism.

5. Excellent colorimetric and fluorometric switchable properties of the molecules suggest that the sensors can be good alternative of traditional pH meters, particularly for the pH detection of alkaline industrial wastes.

6. Applicability of the sensor material was verified over alumina coated plates which revealed that the sensors can utilized as colorimetric pH sensors in solid state.

7. Colorimetric switchability of **1** and **2** through naked eye is considered as the primary advantage of these sensors to be used as a colour changing pH sensor.

III.5. Experimental Section

III.5.1. Material and methods

The reagents were purchased from Aldrich, SD Fine Chemicals and Fluka and used without further purification unless otherwise stated. All the reactions were performed with dried and freshly distilled solvents under anhydrous atmosphere. The precursor compound 9-ethoxy-1-oxophenalene was prepared by following reported procedure [67]. 98% dehydrated ethyl alcohol was used after distillation following reported procedure prior to use in spectroscopic measurement. Doubly distilled water was used throughout the experiments. For the preparation of HEPES buffer system sodium salt of (*4-(2-hydroxyethyl)-1-piperazineethanesulfonic acid* was used in doubly distilled water. The pH of solutions was regulated by adding 1 M HCl for acid range and 1 M NaOH solution for basic range. The compounds were characterized by ^{1}H NMR and ^{13}C NMR and the data were collected from JEOL ECS 400 spectrometer with DMSO-d6 as solvent and tetramethylsilane (TMS) as internal standard. For recording UV-visible absorption spectra were recorded on Agilent 8543 UV-visible spectrophotometer. Fluorescence emission spectra were recorded on PTI spectrofluorometer in steady state mode with FelixGx software. To avoid the entrance of excess stray light 1mm slit width was set for entrance, intermediate and exit slits. Xenon lamp was used as the source of radiation for steady state fluorescence experiments. The structure of compound **1** was optimized with Gaussian 09 software using 6-31G(d, p) basis set on B3LYP level of computation considering singlet state. The final data and optimized structure was thereafter processed on Gauss View software.

III.5.2. Synthesis of the receptors

III.5.2.1. Synthesis and characterization of 9-(4-hydroxyphenyl)-1-oxophenalene (1)

To a stirred solution of 4-aminopheniol (447.4 mg, 4.1 mmol) in methanol (15 mL), 9-ethoxyphenalenone (920 mg, 4.1 mmol) dissolved in 1, 2-dichloroethane (10 mL) was added drop wise over a period of 5 minutes. The resulting solution was refluxed for 10h with continuous stirring affording a reddish orange solution. The solution was filtered upon cooling to room temperature and the crude product was purified by preparative TLC to give an orange solid (**1**), yield 580 mg (49%). UV/vis (DMSO):

λ_{max} [nm] (ε in $M^{-1}cm^{-1}$): 339 (8,577), 357 (14,308), 441 (8,026), 470 (12,706); ESI MS: m/z 288.148 ($M+H^+$). ^1H NMR (DMSO-d_6) in ppm: 6.89-6.93 (m, 3H), 7.2 (d, 2H), 7.3 (d, 1H), 7.5 (t, 1H), 8.05-8.09 (m, 3H), 8.1 (d, 1H), 9.7 (s, 1H, -OH proton), 13.6 (s, 1H, -NH proton),. ^{13}C NMR (DMSO-d_6) in ppm: 108.01, 116.04, 116.84, 122.95, 125.16, 126.98, 128.06, 128.6, 129.22, 132.2, 132.68, 139.08, 139.5, 154.58, 156.58, 184.04. Anal. Calcd. for $C_{19}H_{13}NO_2$: C, 79.43; H, 4.56; N, 4.88. Found: C, 78.8; H, 4.28; N, 4.67.

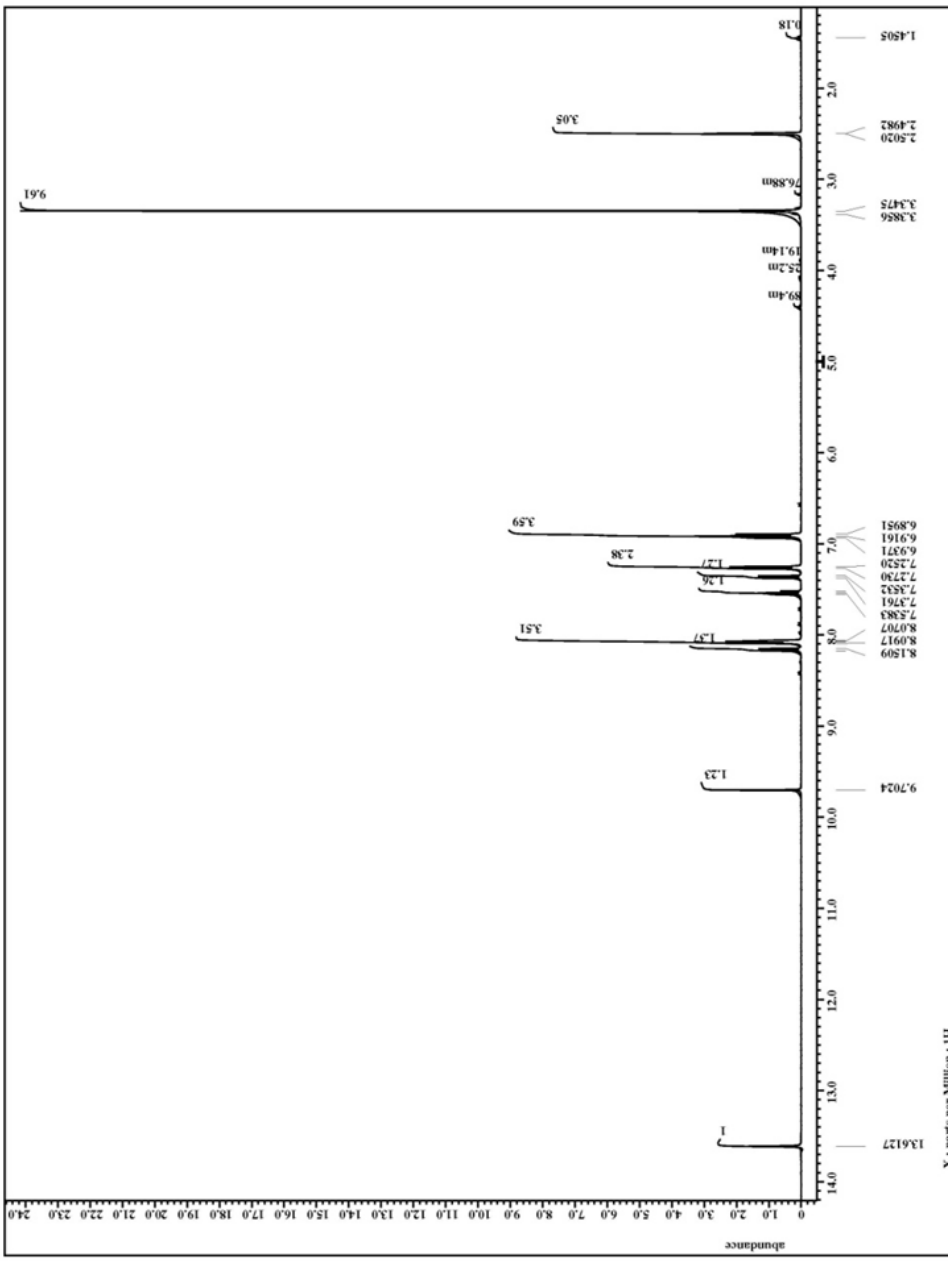

Fig.III.22. ^1H NMR spectra of **1** in DMSO-D6.

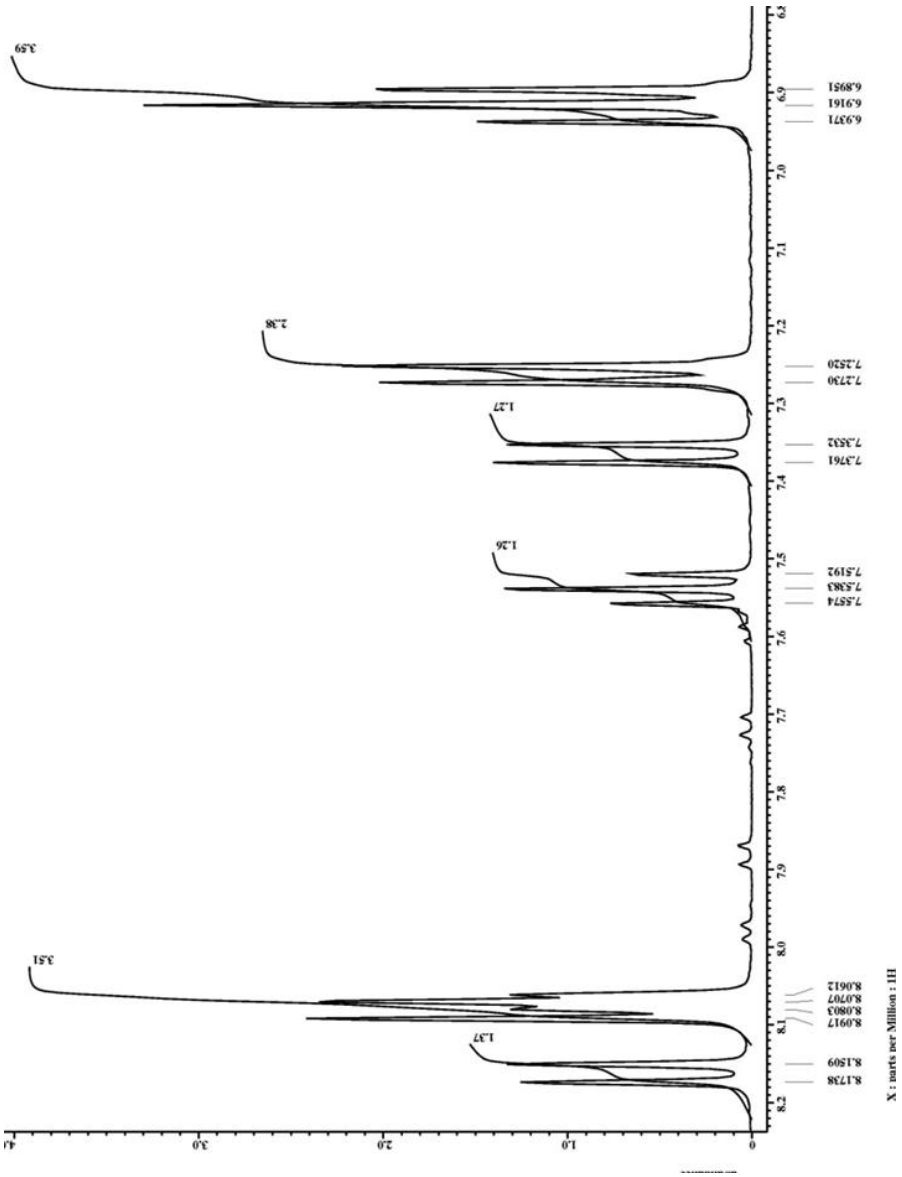

Fig.III.23. Expanded aromatic region in the ^{1}H NMR spectra of **1** in DMSO-D6.

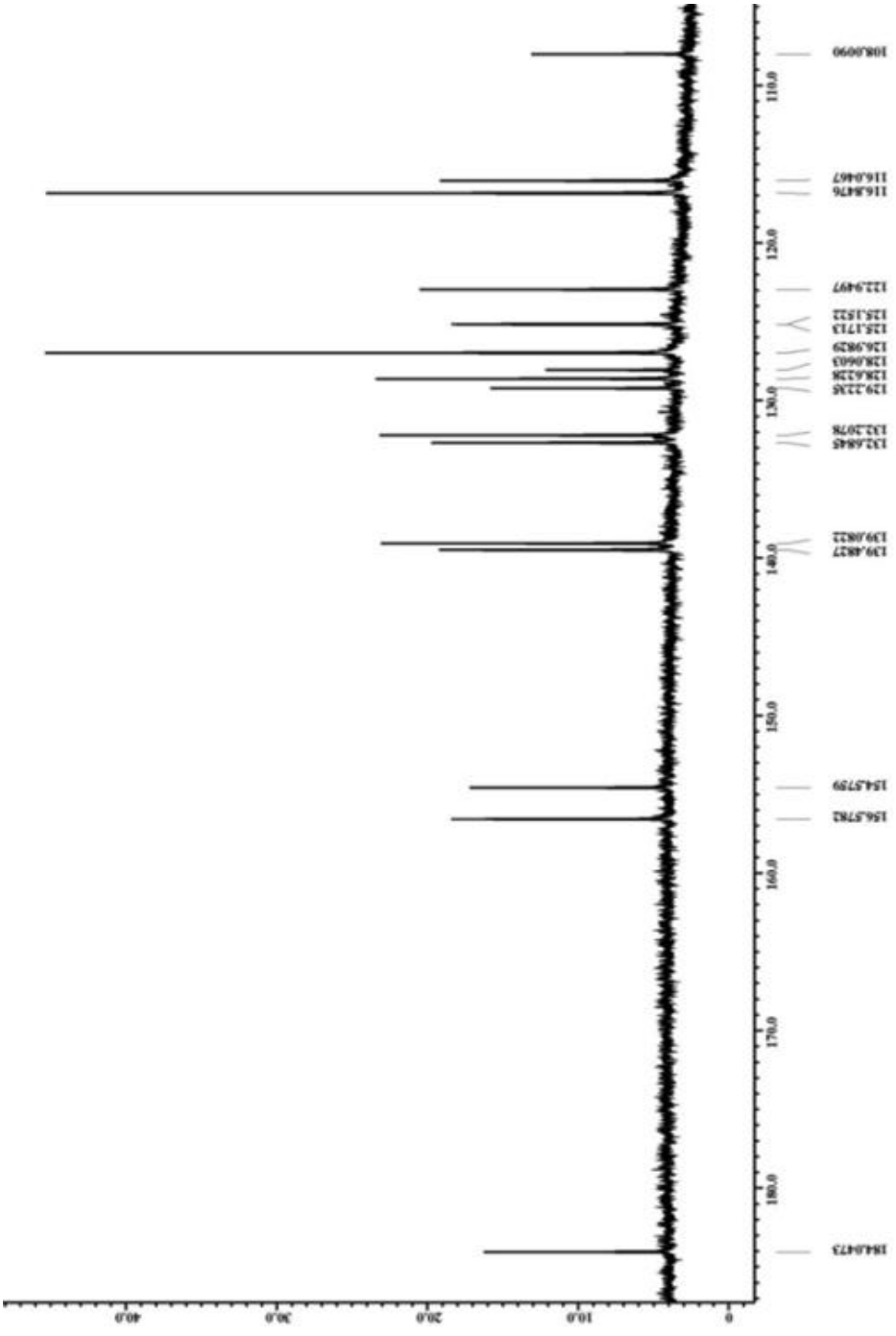

Fig.III.24. ^{13}C NMR spectra of **1** in DMSO-D6.

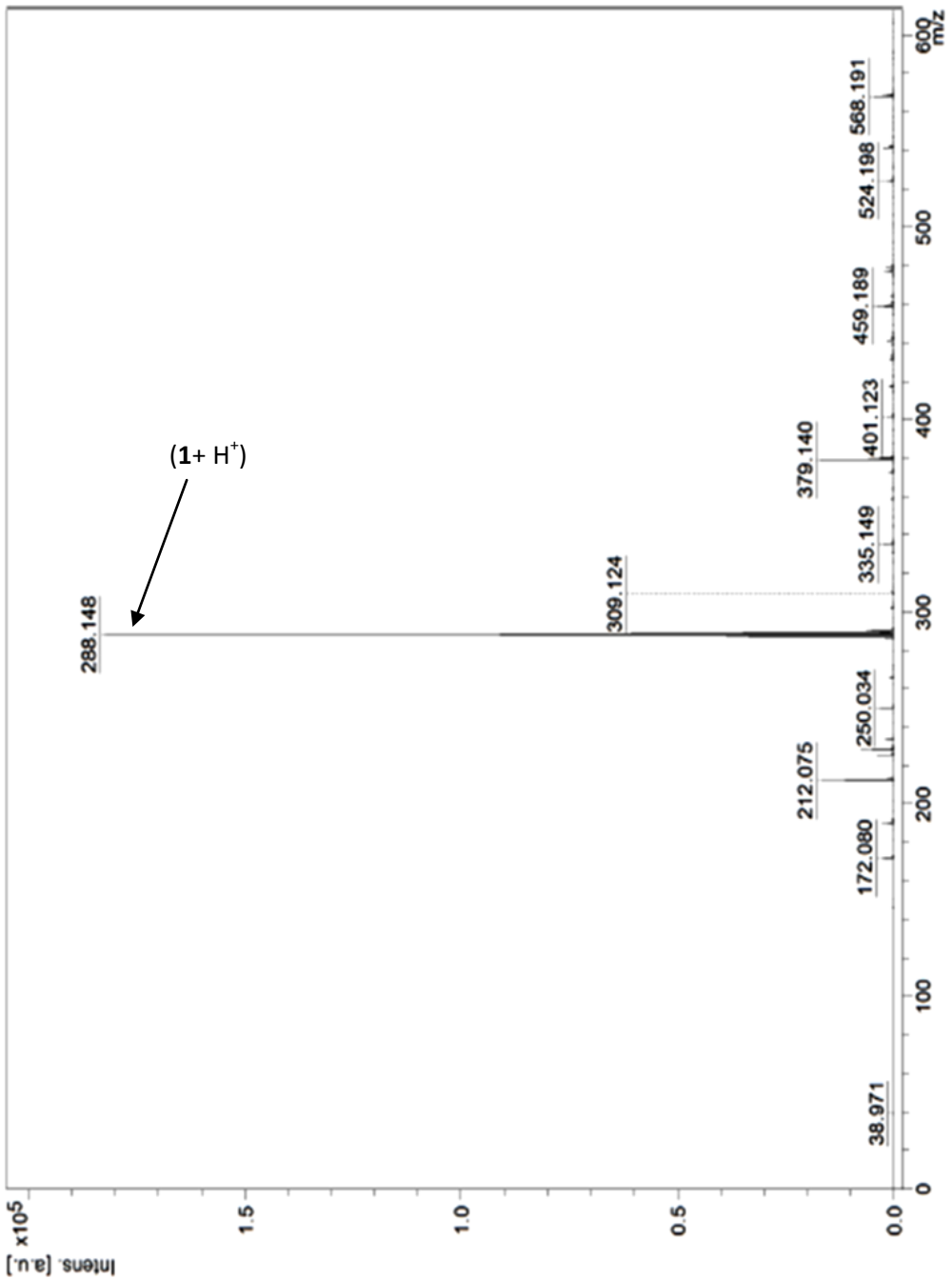

Fig.III.25. ESI Mass spectra of **1** in methanol.

III.4.2.2. Synthesis and characterisation of 2, 2-difluoro-3-(4-hydroxyphenyl)-2-bora-3-aza-1-oxophenalene (2)

To a degassed solution of **1** (0.2 g, 0.698 mmol) in 1,2-dichloroethane (30 mL), $BF_3.Et_2O$ (0.105 mL, 0.831 mmol) was added at 298 K under N_2 atmosphere. The resulting mixture was refluxed at room temperature for 12h in an inert atmosphere. After that the mixture was filtered and the filtrate was removed under vacuum. The orange crude product (380 mg) was then purified by preparative TLC analysis on

Silica gel using 1:1 pet ether/ chloroform mixture as eluent to give a light orange solid (245 mg, 73% yield). UV/vis (DMSO): λ_{max} [nm] (ε in $M^{-1}cm^{-1}$): 253 nm (63,400), 355 (45,950), 446 (26,288), 478 (16,786); ESI MS: m/z 316.157 $(M\text{-}F^{-})^{+}$. ^{1}H NMR (DMSO-d_6) in ppm: 6.879-6.93 (q, 3H), 7.17 (d, 2H), 7.59(d, 1H), 7.1-7.8 (t, 1H), 8.27-8.3 (m, 2H), 8.4 (d, 1H), 8.6 (d, 1H), 9.83 (s, 1H, -OH proton). Anal. Calcd. for $C_{19}H_{12}BF_2NO_2$: C, 68.10; H, 3.61; N, 4.18. Found: C, 67.12; H, 2.98; N, 3.19.

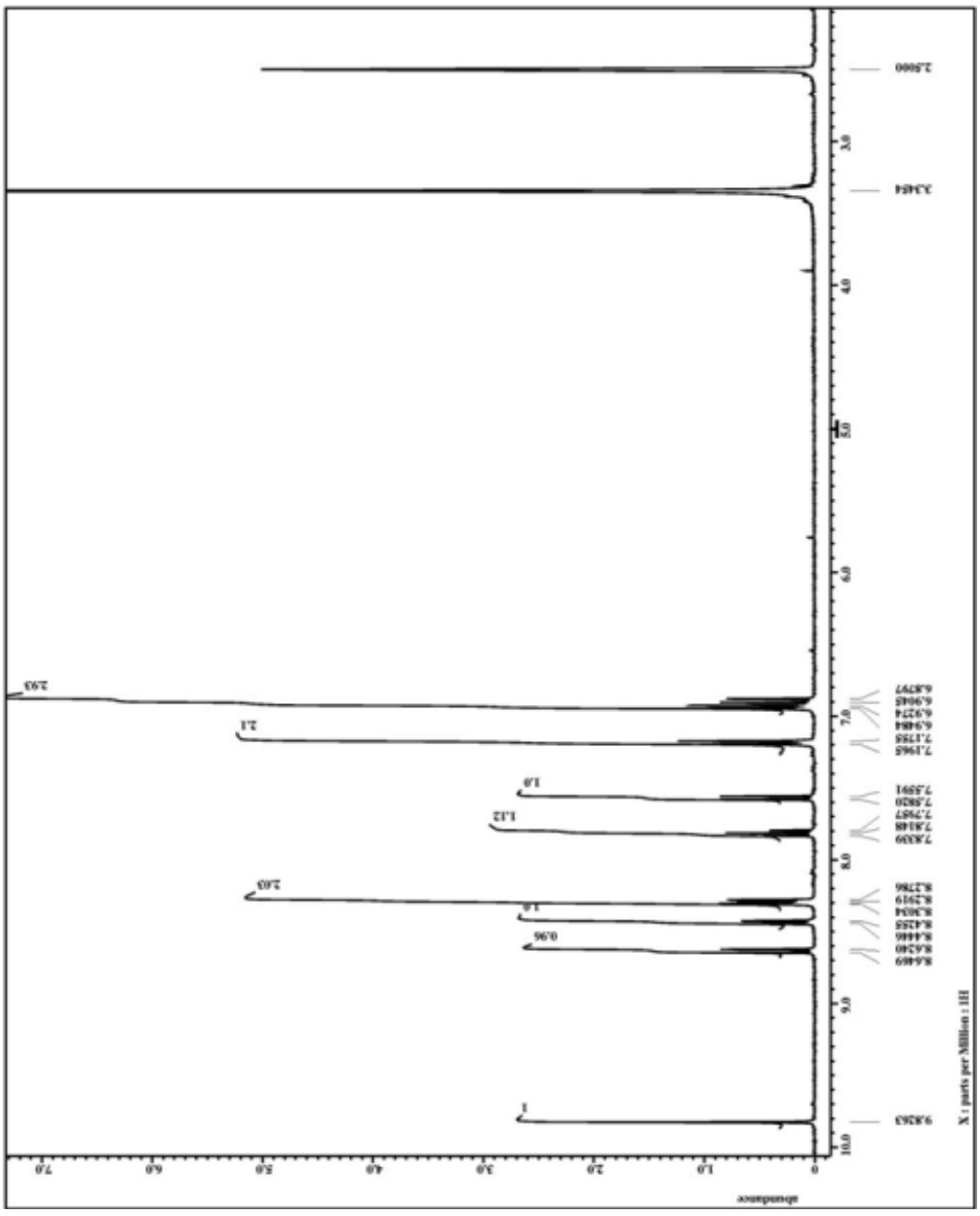

Fig.III.26. ^{1}H NMR spectra of **2** in DMSO-D6.

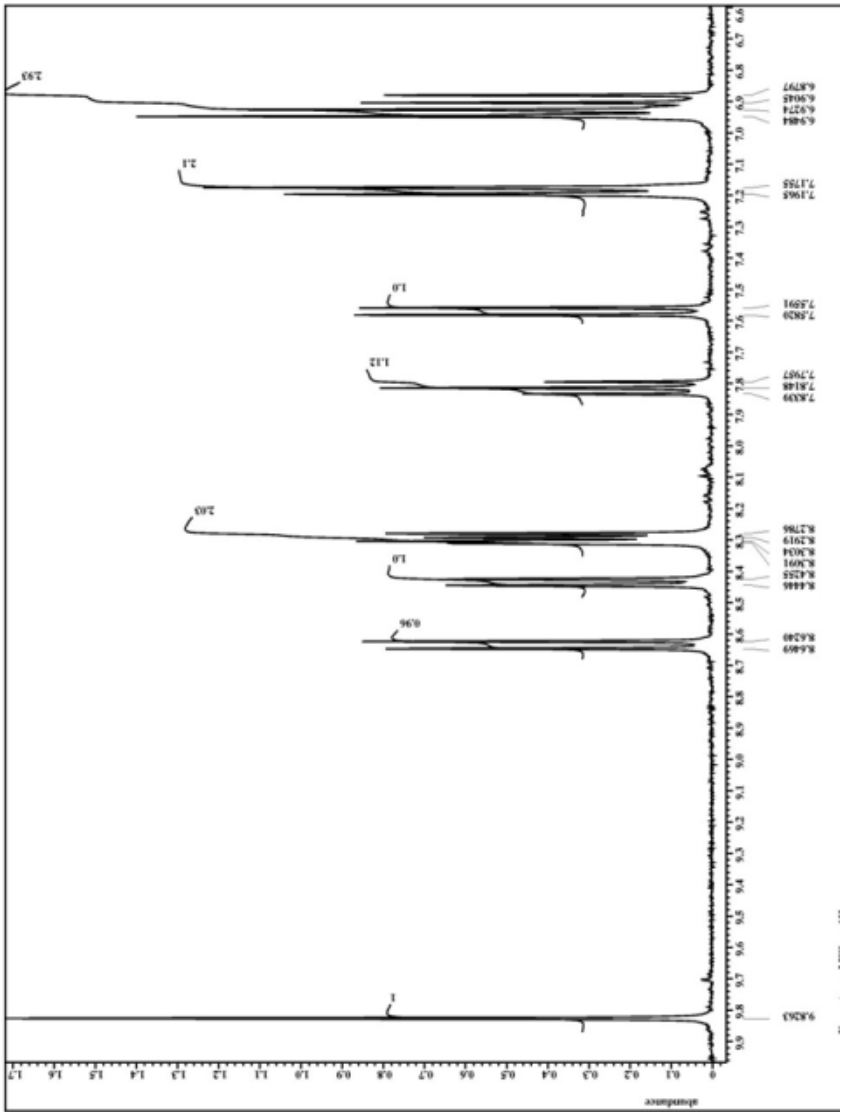

Fig.III.27. Expanded aromatic region in the ^{1}H NMR spectra of **2** in DMSO-D6.

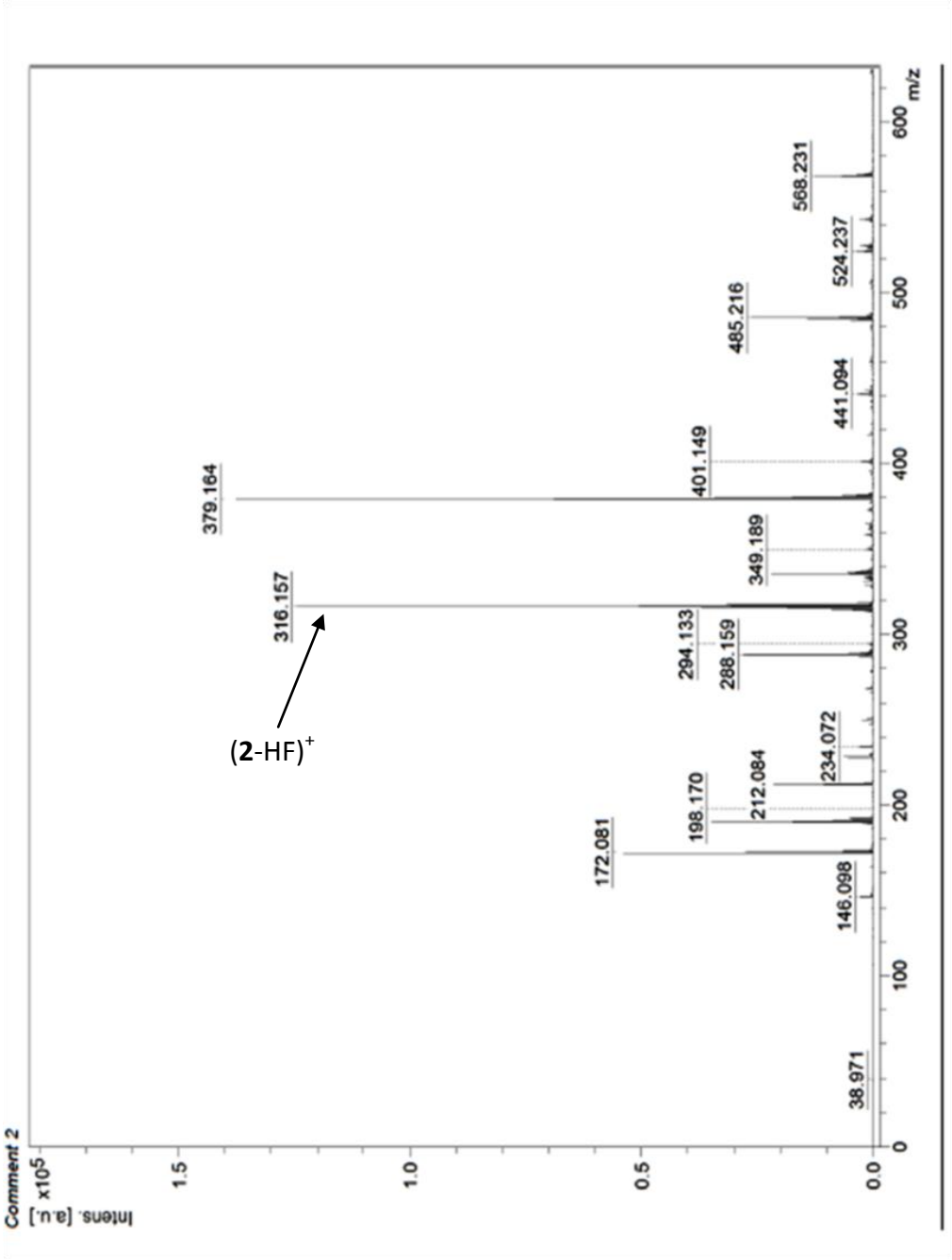

Fig.III.28. ESI mass spectra of **2** in methanol.

III.5.3. General Procedure for spectroscopic experiments

For UV-visible absorption spectral measurements stock solutions of **1** and **2** have been prepared in distilled ethyl alcohol in a concentration of 0.5 mM. In a cuvette 20 µL of 0.5 mM probe solution was taken followed by the addition of 200 µL of 1 M buffer solution, ethanol and water (in 1:1 ration) to make the volume right up to 2 mL, so that the final concentration of the probes is maintained at $5x10^{-6}$ M. Test solutions for emission spectroscopy were also prepared in the same procedure. For

^{1}H NMR experiments 1 mg of **1** was dissolved in 0.6 mL DMSO-d6. NMR spectra at pH 7 were taken with this solution. After recording at pH 7 0.001 mL concentrated HCl was added and spectra was recorded for pH 2. For solution at pH 12, 0.001 mL of 1M NaOH solution was added to the probe solution prepared in DMSO-d6.

III. 6. References

[1] K. P. Carter, A. M. Young, A. E. Palmer, *Chem. Rev*. 2014, **114**, 4564.

[2] N. R. Chereddy, P. M. Nagaraju, V. N. Raju, V. R. Krishnaswamy, P. S. Korrapati, P. R. Bangal, *Biosens. Bioelectron*. 2015, **68**, 749.

[3] E. Tamanini, A. Katewa, L. M. Sedger, M. H. Todd, M. Watkinson, *Inorg. Chem*. 2009, **48**, 319.

[4] J. Li, Q. Hu, X. Yu, Y. Zeng, C. Cao, X. Liu, J. Guo, Z. Pan, *J. Fluoresc.* 2011, **21**, 2005.

[5] R. T. Kennedy, L. Huang, C. A. Aspinwall, *J. Am. Chem. Soc*. 1996, **118**, 1795.

[6] Q. Q. Zhang, M. Zhou, *Talanta*. 2015, **131**, 66.

[7] R. A. Gatenby, R. J. Gillies, *Nat. Rev. Cancer*. 2008, **8**, 56.

[8] H. Izumi, T. Torigoe, H. Ishiguchi, H. Uramoto, Y. Yoshida, M. Tanabe, T. Ise, T. Murakami, T. Yoshida, M. Nomoto, K. Kohno, *Cancer. Treat. Rev*. 2003, **29**, 541.

[9] F. Qu, N. B. Li, H. Q. Luo, *Langmuir*. 2013, **29**, 1199.

[10] M. Tomasulo, I. Yildiz, F. M. Raymo, *J. Phys. Chem. B*. 2006, **110**, 3853.

[11] Y. S. Liu, Y. H. Sun, P. T. Vernier, C. H. Liang, S. Y. C. Chong, M. A. Gundersen, *J. Phys. Chem. C*. 2007, **111**, 2872.

[12] K. Kim, J. W. Lee, J. Y. Choi, K. S. Shin, *Langmuir*. 2010, **26**, 19163.

[13] J. Y. Lei, L. Z. Wang, J. L. Zhang, *Chem. Commun.* 2010, **46**, 8445.

[14] S. Saha, K. Chakraborty, Y. Krishnan, *Chem. Commun*. 2012, **48**, 2513.

[15] X. Chen, X. Y. Cheng, J. J. Gooding, *Analyst*. 2012, **137**, 2338.

[16] V. G. H. Laftte, W. Wang, A. S. Yashina, N. S. Lawrence, *Electrochem. Commun.* 2008, **10**, 1831.

[17] M. Stredánsky, A. Pizzariello, S.; Stredánska, S. Miertu, *Anal. Chim. Acta*. 2000, **415**, 151.

[18] L. Xiong, C. Batchelor-McAuley, R. G. Compton, *Sens. Actuat. B –Chem*. 2011, **159**, 251.

[19] D. A. Skoog, D. M. West, J. Holler, S. R. Crouch, *Fundamentals of Electro-Analytical Chemistry.* 2004.

[20] G. Cui, J. S. Lee, S. J. Kim, H. Nam, G. S. Cha, H. D. Kim, *Analyst*. 1998, **123**, 1855.

[21] G. G. Wildgoose, M. Pandurangappa, N. S. Lawrence, L. Jiang, T. G. J. Jones, R. G. Compton, *Talanta*. 2003, **60**, 887.

[22] M. Lu, R. G. Compton, *Analyst*. 2014, **139**, 2397.

[23] R. B. Moon, J. H. Richards, *J. Biol. Chem*. 1973, **248**, 7276.

[24] D. Wencel, T. Abel, C. McDonagh, *Anal. Chem*. 2014, **86**, 15.

[25] Z. Liu, F. Luo, T. Chen, *Anal. Chim. Acta*. 2004, **510**, 189.

[26] M. Cajlakovic, A. Lobnik, T. Werner, *Anal. Chim. Acta*. 2002, **455**, 207.

[27] A. Lobnik, I. Oehme, I. Murkovic, O. S. Wolfbeis, *Anal. Chim. Acta*. 1998, **367**, 159.

[28] D. A. Nivens, M. V. Schiza, S. M. Angel, *Talanta*. 2002, **58**, 543.

[29] D. Aigner, B. Ungerböck, T. Mayr, R. Saf, I. Klimant, S. M. Borisov, *J. Mater. Chem. C*. 2013, **1**, 5685.

[30] J. L. Hu, F. Wu, S. Feng, J. H. Xu, Z. H. Xu, Y.Q. Chen, T. Tang, X.C. Weng, X. Zhou, *Sens. Actuat. B. -Chem.* 2014, **196**, 194.

[31] H. S. Lv, S. Y. Huang, Y. Xu, X. Dai, J. Y. Miao, B.X. Zhao, *Bioorg. Med. Chem. Lett.* 2014, **24**, 535.

[32] J. Chao, Y. Liu, J. Sun, L. Fan, Y. Zhang, H. Tong, Z. Li, *Sens. Actuat. B-Chem*. 2015, **221**, 427.

[33] M. Baruah, W. Qin, N. Basaric´, W. M. D. Borggraeve, N. Boens, J*. Org. Chem.* 2005, **70**, 4152.

[34] J. Killoran, S. O. McDonnell, J. F. Gallagher, D. F. O'Shea, *New J. Chem*. 2008, **32**, 483.

[35] J. Murtagh, D. O. Frimannsson, D. F. O'Shea, *Org. Lett*. 2009, **11**, 5386.

[36] J. Carrillo, M. Guzmán, *Microchem. J.* 1979, **24**, 234.

[37] G. S. Roadcap, R. A. Sanford, Q. Jin, J. R. Pardianas, C. M. Bethke, *Ground Water*. 2006, **44**, 511.

[38] R. J. Meier, J. M. B. Simbürger, T. Soukka, M. Schäferling, *Chem. Commun.* 2015, **51**, 6145.

[39] J. Lei, L. Wang, J. Zhang, *Chem. Commun*. 2010, **46**, 8445.

[40] Q. Zheng, M. F. Juette, S. Jockusch, M. R. Wasserman, Z. Zhou, R. B. Altman, S. C. Blanchard, *Chem. Soc. Rev*. 2014, **43**, 1044.

[41] J. R. Askim, M. Mahmoudi, K. S. Suslick, *Chem. Soc. Rev*. 2013, **42**, 8649.

[42] F. Carnovale, T.H. Gan, J. B. Peel, K. D. Franz, *JCS Perkin Trans. II*. 1980, 957.

[43] A. Mitra, A. Priyar, S. Bose, P. Bandyopadhyay, A. Sarkar, *Sens. Actuat. B-Chem*., 2015, **210**, 712.

[44] T. Gareis, C. Huber, O. S. Wolfbeis, J. Daub, *Chem. Commun*. 1997, 1717.

[45] J. Killoran, S. O. McDonnell, J. F. Gallagher, D. F. O'Shea, *New J. Chem*. 2008, **32**, 483.

[46] D. Aigner, S. A. Freunberger, M. Wilkening, R. Saf, S. M. Borisov, I. Klimant, *Anal. Chem*. 2014, **86**, 9293.

[47] N. Boens, V. Leen, W. Dehaen, *Chem. Soc. Rev*. 2012, **41**, 1130.

[48] T. Jokic, S. M. Borisov, R. Saf, D. A. Nielsen, M. Kühl, I. Klimant, *Anal. Chem*. 2012, **84**, 6723.

[49] K. D. Franz, *J. Org. Chem.* 1979, **44**, 1704.

[50] W. Yan, X. Wan, Y. Chen, *J. Mol. Structure*. 2010, **968**, 85.

[51] R. A. Bissell, A. P. de Silva, W. T. M. L. Fernando, S. T. T. K. Patuwathavithana, S. D. Samarasinghe, *Tetrahedron Lett.* 1991, **32**, 425.

[52] A. de Silva, T. S. Moody, G. D. Wright, *Analyst*. 2009, **134**, 2385.

[53] A. Jana, P. K. Sukul, S. K. Mandal, S. Konar, S. Ray, K. Das, J. A. Golen, A. L. Rheingold, S. Mondal, T. K. Mondal, A. R. Khuda-Bukhsh, S. K. Kar, *Analyst*. 2014, **139**, 495.

[54] W. Yan, X. Wan, Y. Chen, *J. Mol. Struct*. 2010, **968**, 85.

[55] X. Zhu, Q. Lin, Y.-M. Zhang, T. B. Wei, *Sensor. Actuat. B. Chem*. 2015, **219***,* 38.

[56] M. Hecht, W. Kraus, K. Rurack, *Analyst*. 2013, **138**, 325.

[57] (a) A. Liu, M. Hong, W. Yang, S. Lu, D. Xu, *Tetrahedron*. 2014, **70**, 6974; (b) M. Tian, X. Peng J. Fan, J. Wang, S. Sun, *Dyes and Pigments*. 2012, **95**, 112; (c) Q.-J. Maa, H.-P. Li, F. Yang, J. Zhang, X.-F. Wu, Y. Bai, X.-F. Li, *Sens. Actuat. B-Chem*. 2012, **166– 167**, 68; (c) H.-S. Lv, J. Liu, J. Zhao, B.-X. Zhao, J.-Y. Miao, *Sens. Actuat. B-Chem*. 2013, **177**, 956; (d) L. Liu, P. Guo, L. Chai, Q. Shi, B. Xu, J. Yuan, X. Wang, X. Shi, W. Zhang, *Sens. Actuat.B-Chem*. 2014, **194**, 498.

[58] K. D. Franz, R. L. Martin, *Tetrahedron.* 1978, ***34***, 2147.

[59] H. Li, J. Guo, X. Zhang, Z. Chen, *Heteroatom Chem*. 2012, **23**, 551.

[60] Z. Yang, W. Qin, J. W. Y. Lam, S. Chen, H. H. Y. Sung, I. D. Williams, B. Z. Tang, *Chem. Sci.*, 2013, **4**, 3725.

[61] U. C. Saha, K. Dhara, B. Chattopadhyay, S. K. Mandal, S Mondal, S. Sen, M. Mukherjee, S. van Smaalen, P. Chattopadhyay, *Org. Lett*. 2011, **13**, 4510.

[62] A. D. Becke, *Phys. Rev. A*. 1988, **38,** 3098.

[63] A. D. Becke, *J. Chem. Phys.* 1993, **98**, 5648.

[64] C. Lee, W. Yang, R. G. Parr, *Phys. Rev. B*. 1988, **37**, 785.

[65] J. P. Perdew, *Phys. Rev. B.* 1986, **33**, 8822.

[66] R. C. Haddon, R. Rayford, A. M. Hirani, *J. Org. Chem*. 1981, **46**, 4587.